

# Full simulation study of very light gravitino at the ILC

Ryo Katayama,<sup>1</sup> Takuaki Mori,<sup>1</sup> Keisuke Fujii,<sup>2</sup> Shigeki Matsumoto,<sup>3</sup>  
Taikan Suehara,<sup>4</sup> Tomohiko Tanabe,<sup>4</sup> and Satoru Yamashita<sup>4</sup>

<sup>1</sup>*Department of Physics, The University of Tokyo, Tokyo 113-0033, Japan*

<sup>2</sup>*High Energy Accelerator Research Organization (KEK), Tsukuba 305-0801, Japan*

<sup>3</sup>*Kavli Institute for the Physics and Mathematics of the Universe, Kashiwa 277-8583, Japan*

<sup>4</sup>*International Center for Elementary Particle Physics,  
The University of Tokyo, Tokyo 113-0033, Japan*

We explore the capability of the International Linear Collider (ILC) to measure the mass of a stable gravitino whose mass is in the  $\mathcal{O}(1\text{--}10)$  eV range using full simulation of the ILD detector model. Such gravitino masses typically arise in low-scale gauge mediation scenarios of the supersymmetry breaking. The next-to-lightest supersymmetric particle is chosen to be the stau. Through the measurement of the stau mass and lifetime, the gravitino mass can be determined. We work with the benchmark point of stau mass of  $m_{\tilde{\tau}} = 120$  GeV and stau lifetime of  $c\tau_{\tilde{\tau}} = 100 \mu\text{m}$ . The  $e^+e^- \rightarrow \tilde{\tau}^+\tilde{\tau}^-$  reaction is identified using the one-prong decay of the tau lepton. The main background processes are identified to be  $e^+e^- \rightarrow VV \rightarrow l^+l^-\nu\bar{\nu}$  where  $V = W^\pm$  or  $Z^0$ ,  $e^+e^- \rightarrow \tau^+\tau^-$ ,  $\gamma\gamma$ ,  $e\gamma$ , and Bhabha scattering events. The precision of the stau mass is estimated to be  $\Delta m/m = 0.6\%$  from the threshold scan at  $\sqrt{s} = 250$  GeV with an integrated luminosity of  $100 \text{fb}^{-1}$ , while with the detection of kinematic edge of the tau decay products at  $\sqrt{s} = 500$  GeV assuming an integrated luminosity of  $500 \text{fb}^{-1}$  offers a precision of  $\Delta m/m = 1.4\%$ . The precision of the stau lifetime at  $500 \text{fb}^{-1}$  is estimated to be  $\Delta\tau/\tau = 1.4\%$ , corresponding to the precision of the gravitino mass of 2% when combining with the threshold scan, or 4% when combining with the kinematic edge fit.

## I. INTRODUCTION

Among many new theories beyond the standard model, supersymmetry (SUSY) is a promising candidate in that it can naturally solve the hierarchy problem by canceling the quadratic divergences in the radiative corrections to the Higgs mass parameter with the introduction of supersymmetric particles whose couplings are determined by gauge principles. Moreover, grand unification could be achieved by imposing SUSY. New sources of CP violation and flavor-changing neutral current may arise due to the presence of additional SUSY particles, known as the SUSY flavor problem, many SUSY models incorporate explicit mechanisms to suppress such effects. The gauge-mediated SUSY breaking (GMSB) scenarios [2] naturally solve the SUSY flavor problem by generating SUSY breaking soft mass terms at the messenger scale below the grand unification scale.

In GMSB scenarios with  $R$ -parity conservation, the gravitino appears as the lightest supersymmetric particle (LSP). Taking into account the cosmological data, the gravitino mass can be classified into two regions [3, 4]: the so-called low-scale region corresponds to the gravitino mass of around  $m_{3/2} \approx 1\text{--}10$  eV, while the high-scale region corresponds to  $m_{3/2} \approx 10^6\text{--}10^9$  eV. The low-scale region is not constrained by considerations of the reheating temperature, which makes thermal leptogenesis viable. This is in contrast to the high-scale region which requires low reheating temperatures. The high-scale region is expected to be eventually covered by LHC data, while the low-scale region will remain largely unexplored.

Precision measurements of the gravitino mass, such as those at the International Linear Collider (ILC), can help constrain the SUSY breaking scale. In this study, we

estimate the sensitivity of the ILC to a very light gravitino mass in the GMSB scenario, assuming that the next lightest supersymmetric particle (NLSP) is the stau. We study the stau pair production process  $e^+e^- \rightarrow \tilde{\tau}^+\tilde{\tau}^-$  with the subsequent stau decay  $\tilde{\tau} \rightarrow \tau\tilde{G}$ , whose diagram is shown in Fig. 1. The stau lifetime  $\tau_{\tilde{\tau}}$  can be expressed

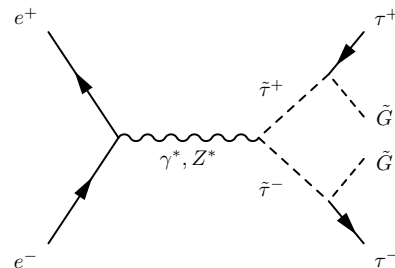


FIG. 1. Feynman diagram for the  $e^+e^- \rightarrow \tilde{\tau}^+\tilde{\tau}^-$  reaction including the stau decay  $\tilde{\tau} \rightarrow \tau\tilde{G}$ .

in terms of the stau mass  $m_{\tilde{\tau}}$  and the gravitino mass  $m_{3/2}$  as follows [5]:

$$\tau_{\tilde{\tau}} = 48 \pi M_{\text{Pl}}^2 m_{3/2}^2 / m_{\tilde{\tau}}^5 \quad (1)$$

where  $M_{\text{Pl}}$  is the Planck scale. In this study, we adopt the following benchmark point: stau mass of  $m_{\tilde{\tau}} = 120$  GeV, and stau lifetime of  $100 \mu\text{m}$ . This corresponds to a gravitino mass of 3.7 eV. Since the observed particles will be the decay products of the tau, which itself decays from the stau, the challenge imposed on the detector is to discriminate the tau decay products whose displacement from the primary interaction point is slightly enhanced by the flight of the stau. In this study, only the one-prong decay of the tau is considered. Thus our primary observ-

able in the lifetime measurement will be the impact parameter of the tau decay products. Our analysis strategy is summarized as follows. First, we determine the precision of the stau mass from the cross section scan near the stau pair production threshold around  $\sqrt{s} \approx 250$  GeV. Then we perform the analysis at  $\sqrt{s} = 500$  GeV for an alternative determination of the stau mass precision through the use of kinematic edges, as well as the stau lifetime measurement from the impact parameter distribution. Finally, we propagate the estimated precision into the gravitino mass via Eq. (1).

The paper is organized as follows. In Sec. II, the signal and background processes are described, along with the simulation framework. We describe the stau mass measurement through the cross section scan in Sec. III and the stau mass measurement from kinematic edges and the lifetime measurement in Sec. IV. We summarize the precision estimates in Sec. V.

## II. SIGNAL AND BACKGROUND PROCESSES

The signal process is stau pair production  $e^+e^- \rightarrow \tilde{\tau}^+\tilde{\tau}^- \rightarrow \tau^+\tau^-\tilde{G}\tilde{G}$ . The left-handed stau is assumed to be heavy. Thus the production is dominated by the right-handed stau. In this study, the tau lepton is reconstructed in the one-prong mode, which corresponds to 85% of its decay. We take advantage of the beam polarizations at the ILC by choosing the right-handed electron and left-handed positron configuration ( $P_{e^-} = +0.8$  and  $P_{e^+} = -0.3$ ) in order to reduce background contributions from SM processes. The following processes are identified as possible background sources:

- $e^+e^- \rightarrow \tau^+\tau^-$
- $e^+e^- \rightarrow VV \rightarrow l^+l^-\nu\bar{\nu}$ , where  $V = W^\pm$  or  $Z^0$
- $e^+e^- \rightarrow e^+e^-$  (Bhabha scattering)
- $e\gamma, \gamma\gamma \rightarrow l^+l^-X, q\bar{q}$

The  $e^+e^- \rightarrow \tau^+\tau^-$  background can be reduced by requiring that the tau pair is back-to-back. The  $e^+e^- \rightarrow VV \rightarrow l^+l^-\nu\bar{\nu}$  processes can be a source of background if the final state contains tau leptons. In particular, the former is an irreducible background because of its event topology is similar to that of the signal. While the beam-related backgrounds  $\gamma\gamma \rightarrow l^+l^-, q\bar{q}$  and Bhabha scattering reactions have different event topologies, their background contribution is nevertheless investigated because their cross sections are large. The cross sections at  $\sqrt{s} = 250$  GeV and 500 GeV for the signal and background processes are summarized in Tab. I.

Signal events are generated using PHYSSIM [6], which calculates the scattering amplitude using HELAS [7], properly taking into account the angular distributions of the decay products. Background samples are generated using WHIZARD [9]. The decay of the tau lepton is handled by TAUOLA [11]. The final state particles are

TABLE I. Cross sections  $\sigma_{\sqrt{s}}$  for signal and background processes for  $\sqrt{s} = 250$  GeV and 500 GeV. The beam polarizations are taken to be  $(P_{e^-}, P_{e^+}) = (+80\%, -30\%)$ .

Process	$\sigma_{100}$ (fb)	$\sigma_{500}$ (fb)
$e^+e^- \rightarrow \tilde{\tau}^+\tilde{\tau}^-$ ( $m_{\tilde{\tau}} = 120$ GeV)	11.3	270.4
$e^+e^- \rightarrow \tau^+\tau^-$	10454.8	1591.2
$e^+e^- \rightarrow VV \rightarrow l^+l^-\nu\bar{\nu}$	4386.0	3341.6
$e^+e^- \rightarrow e^+e^-$ (Bhabha scattering)	$1.73 \times 10^7$	$1.74 \times 10^7$
$e\gamma, \gamma\gamma \rightarrow l^+l^-X, q\bar{q}$ (includes preselection)	$3.58 \times 10^7$	$5.64 \times 10^6$

passed as input to PYTHIA [10]. The effects of initial state radiation and beamstrahlung are included in the event generation.

The detector response is simulated using Mokka, which is based on GEANT4 [12]. The detector model ILD\_00 is used; it consists of a beam pipe, vertex and silicon tracking detectors and a time projection chamber for charged-particle tracking, and highly granular electromagnetic calorimeter (ECAL) and hadronic calorimeter (HCAL) which are placed within a superconducting solenoid which provides a magnetic field of 3.5 T, and a muon detector and tail catcher. In addition, several calorimeter components are placed in the forward regions to provide lepton identification down to very low polar angles.

## III. STAU MASS MEASUREMENT VIA THRESHOLD SCAN

To evaluate the precision of the stau mass measurement, the technique of the threshold scan is used. We have chosen to perform measurements at three center-of-mass energies:  $\sqrt{s} = 250, 256,$  and  $261$  GeV. The assumed integrated luminosity is  $100 \text{ fb}^{-1}$  at each point, making it a total of  $300 \text{ fb}^{-1}$ . The cross sections are shown in Fig. 2. These samples are also fully simulated and reconstructed. The background samples are simulated and reconstructed at  $\sqrt{s} = 250$  GeV; their contributions are assumed to not vary up to  $\sqrt{s} = 261$  GeV.

The following event selection is applied to reduce the background contributions. The visible energy in the event is required to be between 25 GeV and 140 GeV. This suppresses the Bhabha scattering and  $\gamma\gamma$  backgrounds. The number of charged tracks exceeding a transverse momentum of 5 GeV is required to be exactly two. The track pair is required to have opposite charges. The selected tracks are required to have a polar angle of  $|\cos\theta| < 0.82$ . This suppresses Bhabha scattering in the  $t$ -channel process. The difference in the azimuthal angles of the selected tracks is used to impose the requirement of  $\cos(\phi_2 - \phi_1) > -0.90$  to reduce the  $e^+e^- \rightarrow \tau^+\tau^-$  process, in which the tau pair is produced in the back-to-back configuration. Tracks are required to have a large transverse impact parameter significance  $|d_0/\sigma(d_0)| > 4.0$  to enrich the sample with tau decay

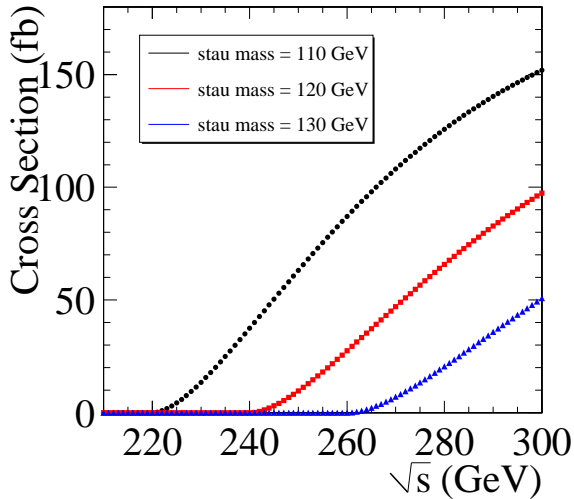


FIG. 2. Cross sections for  $e^+e^- \rightarrow \tilde{\tau}^+\tilde{\tau}^-$  with polarized beams  $(P_{e^-}, P_{e^+}) = (80\%, -30\%)$  for different stau mass.

events. In addition, the missing mass is required to be  $M_{\text{miss}} > 122$  GeV, and the polar angle of the missing momentum direction  $|\cos\theta_{\text{miss}}| < 0.82$ . Lepton identification based on calorimeter energy deposition is applied to reject track pairs which are identified as  $ee$  or  $\mu\mu$ , which suppresses additional SM background. The estimated yields for the event selection are summarized in Tab. II.

Based on the resulting precision of the cross sections, a study of toy Monte-Carlo (MC) experiments is performed to estimate the precision of mass determination. The cross sections of the signal with varying stau mass ( $m_{\tilde{\tau}} = 115, 118, 120, 122, 125$  GeV) are computed at the three center-of-mass energies, to compare against the toy MC experiments. For each toy MC experiment, the signal and background yields are obtained using Poisson statistics. The  $\chi^2$  is computed for each center-of-mass-energy by taking the difference between the measured cross section and the theoretical value, for each stau mass value, divided by the uncertainty of the measured cross section, then squaring it:

$$\chi^2_i = \left( \frac{\sigma_i^{\text{exp}} - \sigma_i^{\text{th}}}{\Delta\sigma_i^{\text{exp}}} \right)^2, \quad i = 250, 256, 261 \text{ GeV} \quad (2)$$

The  $\chi^2$  values as a function of the stau mass are then fit to a parabolic curve to extract the minimum value corresponding to the stau mass estimate. The toy MC is repeated 10,000 times; the resulting stau mass distribution is fit to a Gaussian curve as shown in Fig. 3 to extract the stau mass precision of 0.7 GeV (0.6%).

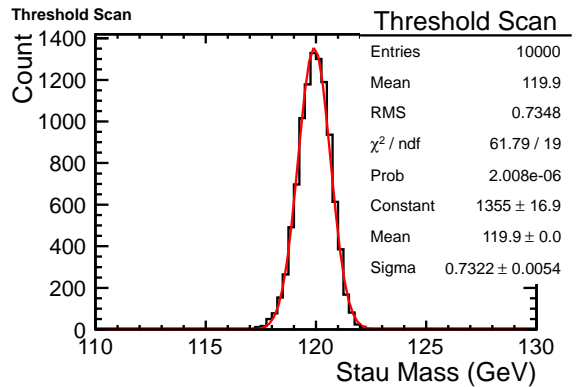


FIG. 3. Result of toy MC for the threshold scan.

#### IV. STAU MEASUREMENTS AT 500 GEV

The strategy to measure the stau lifetime is through the impact parameter distribution of the tau decay products. We choose  $\sqrt{s} = 500$  GeV as the center-of-mass energy for this analysis, as the boost of the stau helps in determining its lifetime. An alternative way to obtain the stau mass through the detection of the kinematic edges of the stau decay products is also presented. While the precision obtained from this method is not expected to exceed that from the cross section scan, the kinematic edge method does not require additional data taking and thus offers a complementary way to determine the mass. The assumed integrated luminosity is  $500 \text{ fb}^{-1}$ . The event selection follows similarly to the threshold scan analysis.

##### A. Common event selection

We describe the event selection procedures which pertain to both the kinematic edge analysis and the lifetime analysis. The visible energy in the event is required to be greater than 50 GeV to suppress  $\gamma\gamma$  backgrounds. The number of reconstructed tracks is required to be two, with opposite charges, each having transverse momentum greater than 5 GeV, to further suppress  $\gamma\gamma$  backgrounds. The polar angle of each track is required to be  $|\cos\theta| < 0.8$  to reduce the Bhabha scattering events. The difference in the azimuthal angles is required to be  $\cos(\phi_2 - \phi_1) > -0.93$  to suppress the tau pair events. In order to discriminate the signal events from SM backgrounds, the following requirement based on the visible energy and the 3-dimensional angle  $\theta_{3D}$  between the two tracks is imposed:  $\theta_{3D}/E_{\text{vis}} > 3^\circ/450 \text{ GeV}$ . The estimated yields of the event selection are summarized in Tab. III, assuming an integrated luminosity of  $500 \text{ fb}^{-1}$  and beam polarizations  $(P_{e^-}, P_{e^+}) = (+0.8, -0.3)$ .

TABLE II. Estimated yields in the threshold scan analysis at  $\sqrt{s} = 250$  GeV, normalized to an integrated luminosity of  $250 \text{ fb}^{-1}$  with beam polarizations  $(P_{e^-}, P_{e^+}) = (+0.8, -0.3)$ .

	$\tilde{\tau}^+\tilde{\tau}^-$ ( $m_{\tilde{\tau}} = 250$ GeV)	$\tilde{\tau}^+\tilde{\tau}^-$ ( $m_{\tilde{\tau}} = 256$ GeV)	$\tilde{\tau}^+\tilde{\tau}^-$ ( $m_{\tilde{\tau}} = 261$ GeV)	$\tau^+\tau^-$	$\gamma\gamma, e\gamma, e^+e^-$	$VV \rightarrow l^+l^-\nu\bar{\nu}$
1. No cut	970	$2.00 \times 10^3$	$2.94 \times 10^3$	$8.04 \times 10^5$	–	$3.72 \times 10^4$
2. Preselection	–	–	–	–	$1.13 \times 10^8$	–
3. Number of tracks = 2	310	645	922	$8.44 \times 10^3$	$3.63 \times 10^5$	$9.87 \times 10^3$
4. Strong preselection	238	505	731	$3.84 \times 10^3$	$1.23 \times 10^4$	$6.87 \times 10^3$
5. $E_{\text{vis}} < 140$ GeV	238	503	726	$1.02 \times 10^3$	$7.22 \times 10^4$	$5.53 \times 10^3$
6. $ \cos \theta_{\text{mis}}  < 0.82$	227	482	694	580	$1.03 \times 10^3$	$5.06 \times 10^3$
7. $M_{\text{mis}} > 122.4$ GeV	208	436	629	165	755	$2.91 \times 10^3$
8. Lepton identification	178	387	548	138	358	$1.80 \times 10^3$
9. $ d_0/\sigma(d_0)  > 4.0$ for each track	122	270	383	70.4	5.3	163

TABLE III. Estimated yields in the 500 GeV analysis, normalized to an integrated luminosity of  $500 \text{ fb}^{-1}$  with beam polarizations  $(P_{e^-}, P_{e^+}) = (+0.8, -0.3)$ .

	$\tilde{\tau}^+\tilde{\tau}^-$	$\tau^+\tau^-$	$\gamma\gamma, e\gamma, e^+e^-$	$VV \rightarrow l^+l^-\nu\bar{\nu}$
1. No cut	$6.81 \times 10^4$	$6.34 \times 10^5$	–	$2.08 \times 10^5$
2. Preselection	–	–	$4.74 \times 10^7$	–
3. Number of tracks = 2	$4.57 \times 10^4$	$3.08 \times 10^5$	$2.19 \times 10^7$	$9.67 \times 10^4$
4. $p_T > 5$ GeV for each track	$3.36 \times 10^4$	$2.28 \times 10^5$	$7.49 \times 10^6$	$8.30 \times 10^4$
5. $E_{\text{vis}} > 50$ GeV	$3.05 \times 10^4$	$2.25 \times 10^5$	$4.06 \times 10^6$	$8.25 \times 10^4$
6. $ \cos \theta  < 0.8$ for each track	$2.50 \times 10^4$	$1.21 \times 10^5$	$2.92 \times 10^6$	$1.96 \times 10^4$
7. $\cos(\phi_2 - \phi_1) > -0.93$	$1.49 \times 10^4$	$9.15 \times 10^3$	$2.71 \times 10^6$	$1.07 \times 10^4$
8. $\theta_{3D}/E_{\text{vis}} > 3.0^\circ/450$ GeV	$1.46 \times 10^4$	$1.06 \times 10^3$	$9.21 \times 10^5$	$7.44 \times 10^3$
<i>Selections 1–8 are common to both analyses at 500 GeV.</i>				
9. $ \cos \theta_{\text{mis}}  < 0.9$	$1.44 \times 10^4$	779	$3.25 \times 10^3$	$7.11 \times 10^3$
10. Lepton identification (loose)	$1.20 \times 10^4$	560	129	$1.65 \times 10^3$
<i>Selections 1–10 are used for the lifetime measurement.</i>				
A. $ d_0/\sigma(d_0)  > 1.0$ for each track	$1.38 \times 10^4$	753	$8.25 \times 10^4$	$1.07 \times 10^3$
B. $ \Delta E_{\text{jet}}  > 100$ GeV	$2.31 \times 10^3$	570	$5.95 \times 10^4$	301
C. Lepton identification (loose)	$2.14 \times 10^3$	404	$1.13 \times 10^4$	132
D. $180 < E_{\text{trk}} < 250$ GeV	201	0.0	0.0	85.6
E. Lepton identification (tight)	186	0.6	0.0	0.3
<i>Selections 1–8 and A–E are used for the mass determination via kinematic edges.</i>				
<i>Selections D and E are applied to individual tracks.</i>				

## B. Stau lifetime determination

Additional selections are imposed for the analysis of the stau lifetime. The angle of the missing momentum is required to be  $|\cos \theta_{\text{miss}}| < 0.9$  for the suppression of  $\gamma\gamma$  and Bhabha scattering events. The energy depositions in the ECAL and HCAL are used to identify leptons; the event configuration with  $ee$  or  $\mu\mu$  are rejected to further reduce SM backgrounds. The estimated yields of the event selection are summarized in Tab. III.

We investigate the stau lifetime determination method which takes exploits the dependence the transverse impact parameter distribution on the stau lifetime. The transverse impact parameter distribution after the event selection is shown in Fig. 4 for a stau mass of 120 GeV and lifetime of  $c\tau = 100 \mu\text{m}$ . High statistics signal samples with various stau lifetime are generated and simulated for

the purpose of template fits. The template samples are chosen to have lifetimes of  $c\tau = (90, 95, 100, 105, 110) \mu\text{m}$ . The expected backgrounds are included, as shown in Fig. 4, for the case of  $c\tau = 100 \mu\text{m}$ . We perform toy MC experiments, each experiment consisting of distributions based on the  $c\tau = 100 \mu\text{m}$  sample with Poisson statistics folded in, according to the number of events expected for an integrated luminosity of  $500 \text{ fb}^{-1}$ . The resulting events are put into a histogram of  $N = 200$  bins, which are then compared against the template samples, to compute the  $\chi^2$  quantity, defined as

$$\chi^2 = \sum_{i=1}^N \left( \frac{n_i^{\text{exp}} - n_i^{\text{templ}}}{\Delta n_i^{\text{exp}}} \right)^2 \quad (3)$$

where  $N$  is the number of bins, and  $n_i^{\text{exp}}$  ( $n_i^{\text{templ}}$ ) is the number of events in the  $i$ -th bin for the experiment (tem-

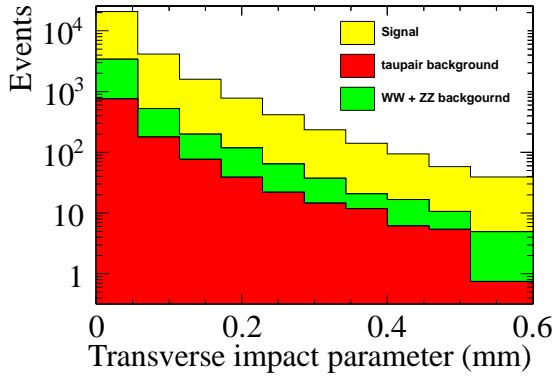


FIG. 4. The transverse impact parameter distributions for signal and background processes after the event selection. Each events contains two tracks, each of which carries a weight of 0.5.

plate) sample. The  $\chi^2$  is computed for the five template samples corresponding to the five different stau lifetime. The  $\chi^2$  points are fit to a parabolic curve, whose minimum is used as the estimate of the stau lifetime for this experiment. The toy MC experiments are performed 10,000 times. We extract the expected precision for stau lifetime from the resulting distribution of the  $\chi^2$  minima. As a result, it is 1.4% for an integrated luminosity of  $500 \text{ fb}^{-1}$  and beam polarizations of  $(P_{e^-}, P_{e^+}) = (+0.8, -0.3)$ .

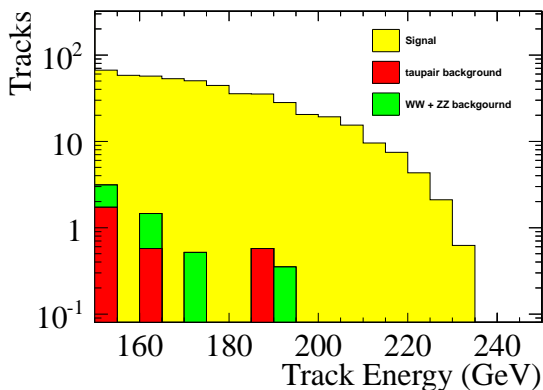


FIG. 5. Track energy distributions for signal and background processes after the event selection.

### C. Stau mass determination via kinematic edges

The event selection is reoptimized for the stau mass measurement through kinematic edges. Starting with the common sample as described in Sec. IV A, additional requirements are imposed as follows. The requirement on the transverse impact parameter significance

$|d_0/\sigma(d_0)| > 1.0$  is used to suppress discrimination of signal and background events. A tight lepton identification is applied. The fit region in the track energy is restricted to be in the range of  $150 < E_{\text{trk}} < 250 \text{ GeV}$ . Furthermore, the energy of the track and the surrounding neutral clusters as identified by jet finders with the number of jets  $N_{\text{jet}} = 2$  is used to discriminate the heavy mass of stau from lighter SM particles by placing a requirement on the difference in the energy such that  $|\Delta E_{\text{jet}}| > 100 \text{ GeV}$ . The estimated yields are summarized in Tab. III.

The mass distribution is modeled via the following function

$$f(x) = \alpha(\beta - x) \exp(-\gamma x) \theta(\beta - x) \quad (4)$$

where  $\alpha$ ,  $\beta$ , and  $\gamma$  are fit parameters constrained to be positive, and  $\theta(x)$  is the Heaviside step function to ensure positivity along the mass distribution. The value of  $\beta$  is used to extract the edge position. Again, toy MC experiments are performed to estimate the precision of the stau mass determination. The result is  $\Delta m/m = \Delta\beta/\beta = 1.4\%$  for an integrated luminosity of  $500 \text{ fb}^{-1}$  and beam polarizations of  $(P_{e^-}, P_{e^+}) = (+0.8, -0.3)$ . This result however depends on the stau lifetime having  $100 = \mu\text{m}$  as we have applied the requirement on the transverse impact parameter.

## V. CONCLUSIONS

In this study, we have looked at the low-scale GMSB scenario with  $R$ -parity conservation and the stau as the NLSP, working with the stau mass of  $120 \text{ GeV}$  and lifetime of  $c\tau = 100 \mu\text{m}$  as a benchmark point. Throughout this study, the beam polarizations are assumed to be  $(P_{e^-}, P_{e^+}) = (+80\%, -30\%)$ . The precision of stau mass was evaluated for one-prong tau decays at two different energies:  $\sqrt{s} = 250$  and  $500 \text{ GeV}$ . In the former case, the mass is determined through the scan of cross section near the threshold; its precision is found to be  $0.6\%$  with an integrated luminosity of  $250 \text{ fb}^{-1}$ . In the latter case, the kinematic edge of the decay products is used; the precision is found to be  $1.4\%$  with an integrated luminosity of  $500 \text{ fb}^{-1}$ . The precision of the stau lifetime determined from the impact parameter distribution at  $\sqrt{s} = 500 \text{ GeV}$  is found to be  $1.4\%$  with an integrated luminosity of  $500 \text{ fb}^{-1}$ . This translates to the precision of the gravitino mass of  $1.7$  ( $3.6\%$ ) when combining the lifetime determination with the mass from the threshold scan (kinematic edge). These numbers take into account only the statistical uncertainty. The determination of the stau lifetime using three-prong decays of the tau lepton should be attempted in future studies.

## VI. ACKNOWLEDGMENTS

The authors would like to thank T. Moroi, and the members of the ILC Physics Working Group for valu-

able discussions. This work was supported in part by the Grant-in-Aid for Specially Promoted Research

No. 23000002 by the Japan Society for Promotion of Science.

- 
- [1] K. A. Intriligator and N. Seiberg, *Class. Quant. Grav.* **24**, S741 (2007).
  - [2] M. Dine and A. E. Nelson, *Phys. Rev. D* **48**, 1277 (1993); M. Dine, A. E. Nelson and Y. Shirman, *Phys. Rev. D* **51**, 1362 (1995); M. Dine, A. E. Nelson, Y. Nir and Y. Shirman, *Phys. Rev. D* **53**, 2658 (1996).
  - [3] T. Moroi, hep-ph/9503210.
  - [4] S. Shirai, M. Yamazaki and K. Yonekura, *JHEP* **1006**, 056 (2010) [arXiv:1003.3155 [hep-ph]].
  - [5] S. Matsumoto and T. Moroi, *Phys. Lett. B* **701**, 422 (2011) [arXiv:1104.3624 [hep-ph]].
  - [6] <http://www-jlc.kek.jp/subg/offl/physsim/>.
  - [7] H. Murayama, I. Watanabe, and K. Hagiwara, , KEK Report No. 91-11 (1992).
  - [8] S. Kawabata, *Comput. Phys. Commun.*, **41**, 127 (1986).
  - [9] W. Kilian, T. Ohl and J. Reuter, *Eur. Phys. J. C* **71**, 1742 (2011) [arXiv:0708.4233 [hep-ph]].
  - [10] T. Sjostrand, L. Lonnblad, S. Mrenna and P. Z. Skands, hep-ph/0308153.
  - [11] S. Jadach, Z. Ws, R. Decker, JH. Kuehn, *Comp. Phys. Comm.* **76** 361 (1993).
  - [12] S. Agostinelli et al. [GEANT4 Collaboration], "GEANT4: A simulation toolkit," *Nucl.Instrum. Meth. A* **506** (2003) 250.
  - [13] J.-C. Brient and H. Videau, (2002), arXiv:hep-ex/0202004.